Photonic band structure of ZnO photonic crystal slab laser

A. Yamilov,[a)] X. Wu, and H. Cao
Department of Physics and Astronomy, Northwestern University, Evanston, Illinois 60208

We recently reported on the realization of ultraviolet photonic crystal laser based on zinc oxide [Appl. Phys. Lett. **85**, 3657 (2004)]. Here we present the details of structural design and its optimization. We develop a computational supercell technique that allows a straightforward calculation of the photonic band structure of ZnO photonic crystal slab on sapphire substrate. We find that despite the small index contrast between the substrate and the photonic layer, the low-order eigenmodes have predominantly transverse-electric (TE) or transverse-magnetic polarization. Because emission from ZnO thin film shows a strong TE preference, we are able to limit our consideration to TE bands, spectrum of which can possess a complete photonic band gap with an appropriate choice of structure parameters. We demonstrate that the geometry of the system may be optimized so that a sizable band gap is achieved. © *2005 American Institute of Physics.*
[DOI: 10.1063/1.2134880]

I. INTRODUCTION

A photonic crystal slab (PhCS) is a layer of dielectric where refractive index is periodically modulated within the plane of the slab.[1–3] Such devices have attracted much attention because of their potential applications to various optoelectronic devices and circuits.[4–10] PhCS may lead to a complete photonic band gap for the guided modes when the wave propagation in all in-plane directions is forbidden due to Bragg interference. Moreover, its planar geometry makes it easy to incorporate on a chip, as well as offers a possibility of low-threshold[5,11–15] electrically driven compact laser source.[16] Defect cavities in these photonic devices can have a high-quality factor and small modal volume.[8,17–19] So far the experimental efforts mainly concentrated on the PhCS made of III-V semiconductors.[5,11–16] They operate in the infrared (IR) communication frequencies (see also Ref. 20), where the structural feature size is on the scale of 0.25 μm.

There is technological and commercial demands for compact and integrable laser sources in the near-ultraviolet (UV) range of optical spectrum. Recently, we reported the realization of an UV PhCS laser that operates at room temperature.[21] This required overcoming of several experimental and design challenges.

First of all, because of the shorter wavelength, PhCS requires smaller structural features with a sub-100-nm size. The fabrication of such miniature structures is technologically challenging for commonly used wide-band-gap semiconductors such as GaN and ZnO. Compared with the other wide-band-gap materials, ZnO has the advantage of large exciton binding energy ($\sim$60 meV), which allows efficient excitonic emission even at room temperature.[22] Using focused ion-beam (FIB) etching technique[21] we were able to achieve more than a fourfold reduction, compared to IR PhCS, of the feature size in ZnO (see also Ref. 23).

Secondly, high-quality ZnO films are usually grown on the lattice-matched sapphire substrate,[24] which results in a relatively low refractive index contrast between PhCS and the substrate. Furthermore, as we detail below, the substrate-PhCS-air geometry rather a air-PhCS-air geometry in the vertical direction disallows the classification of the photonic modes into symmetric and antisymmetric with respect to reflection in the mid-PhCS plane.[3,7,25] Separation of the guided modes according to their symmetry in IR PhCS is usually ensured due to "undercutting," i.e., removing the material directly below the photonic layer.[5,15,16] The separation can also be approximately[7,26] done for systems with a large index contrast between the substrate and PhCS. Neither option is readily available for ZnO-based structures, due to its material properties. At first glance, this makes photonic band gap (PBG) unattainable in our system. The purpose of this paper is to design a ZnO-based PhCS, which exhibits PBG effects.

In Sec. II we introduce a computational supercell technique that allows the calculation of photonic band structure of PhCS on a dielectric substrate. Then we present the detailed analysis of the symmetry and polarization of the photonic modes belonging to different bands. We show that low-order photonic bands can still be approximately classified as TE and TM. In Sec. III we make use of the experimental fact that PhCS is made of a single-crystalline hexagonal ZnO thin film, which is grown along the *c*-crystallographic axis.[24] Since the polarization of exciton emission in the ZnO thin film is predominantly perpendicular to the *c* axis,[27,28] the emission goes preferably into TE-polarized photonic modes. Coincidentally, the air-holes-in-a-dielectric PhCS configuration can possess a complete PBG (with certain parameters) for, namely, TE-polarized modes. Therefore, we consider only TE-polarized photonic modes in our band-structure calculation. Finally, in Sec. IV we systematically study the position and size of the PBG as a function of geometrical parameters: air-hole radius r, slab thickness t_{PhCS}, and etch depth t_e, as illustrated in Fig. 1. We conclude our paper with a discussion section.

[a)]Present address: Department of Physics, University of Missouri-Rolla, Rolla, MO 65409; electronic mail: yamilov@umr.edu
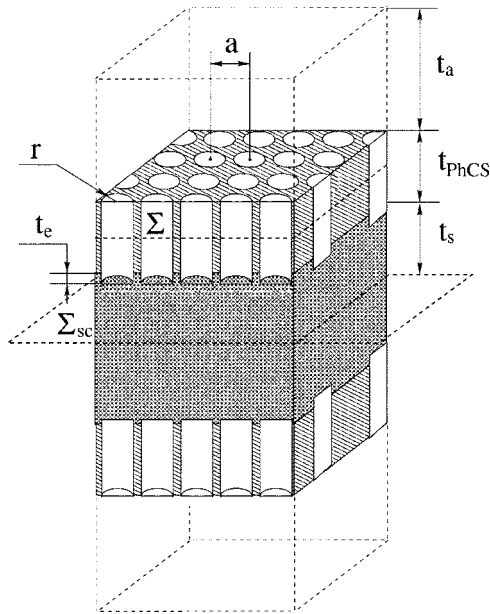
FIG. 1. Schematic diagram of the vertical supercell used in the photonic band-structure simulation. Cylindrical air holes of radius r are arranged in a hexagonal pattern with lattice constant, a. The holes extend throughout the slab of thickness t_{PhCS} and may penetrate into the substrate to the depth of t_e. The thicknesses t_a and t_s need to be chosen sufficiently large. The cell is symmetric with respect to reflection in the Σ_{sc} plane. For convenience we also introduce a middle plane of the slab, Σ.

II. SUPERCELL PHOTONIC BAND-STRUCTURE CALCULATION

Although "Bragg reflection" plus "index-guiding" description of the electromagnetic field in PhCS can elucidate many physical phenomena that occur in such system, it is naive because both in-plane and vertical propagations or confinements are inseparable. In order to obtain the photonic modes of PhCS one needs to solve the problem self-consistently within the same framework. This can be done with a plane-wave expansion method[29] that *de facto* became a standard in the field.

PhCSs designed for IR applications have an inherently large size of the structural units owing to relatively long wavelengths involved. In these systems it is possible to fabricate PhCSs cladded with air above and below (see, e.g., Refs. 5, 15, and 16). This design is advantageous for a number of reasons. First, this is a symmetric structure—there exists a reflection symmetry with respect to the plane that goes through the middle of the PhCS. This symmetry allows two orthogonal classes of eigenfunctions of Maxwell equations: symmetric and antisymmetric.[3] Supercell for the band-structure calculation can be easily constructed by repeating ···-air-PhCS-air-PhCS-··· indefinitely in the vertical direction.[3] It was shown that low-lying (E-field) symmetric modes are predominantly TE polarized, while antisymmetric ones are TM polarized. Due to superior guiding properties of TE modes and the fact that a self-supporting membrane percolated by air holes (unlike the collection of dielectric cylinders in air) exhibits a PBG for the same polarization, this geometry is widely used in practice. The supercell photonic band-structure calculations also give unphysical modes that do not correspond to the guided modes of the PhCS (con-

fined to the slab). Fortunately, physical (guided) modes can be separated using the concept of light cone as follows. In the result of photonic band-structure calculation one obtains the frequency ω for a given in-plane wave vector $\mathbf{k}_{\parallel}$. This electromagnetic (em) mode (concentrated inside the photonic layer) is coupled only to the modes outside the layer with the same $(\omega, \mathbf{k}_{\parallel})$. If $\omega < ck_{\parallel}$, then $k_z = \sqrt{\omega^2/c^2 - k_{\parallel}^2}$ is imaginary outside the PhCS. Thus the light intensity decays exponentially in the z direction away from the layer. This describes a guided mode. In the opposite case, k_z is real and light can escape to the infinity. Such a mode is a leaky mode, which cannot be accurately described in the supercell calculations. A continuum of modes with $\omega > ck_{\parallel}$ form a light cone (a cone in ω-k space). Therefore, PBGs obtained in all planar geometries are, strictly speaking, photonic band gaps for guided modes.

In our UV PhCS laser[21] we used ZnO because of its wide electronic band gap and robustness of the optical properties with respect to damage caused by FIB. There are two consequences relevant for the band-structure calculation. First of all, in order to produce high-quality films, ZnO was grown epitaxially on a sapphire substrate with a *large* refractive index $n_s = 1.78$. Second, our choice of the materials and miniature structure dimensions does not currently allow for removal of the underlying layer of sapphire—undercutting is *impossible*. These experimental limitations lead to severe restrictions. (i) The presence of the sapphire substrate lifts the reflection symmetry.[3] This results in mixing between TE-like and TM-like classes of electromagnetic modes. One may expect that this effect should be large in view of the relatively small index contrast between sapphire and ZnO ($n_{ZnO} = 2.35$). Below we will show that this expectation is not completely borne out. (ii) The most stringent restriction is imposed by the presence of the second light cone—which reflects the possibility of radiative escape into the sapphire substrate. Indeed, although light leakage into the air occurs for $\omega > ck_{\parallel}$, leakage into the substrate starts already for $\omega > (c/n_s)k_{\parallel}$. Avoiding this problem requires the use of a high filling fraction in ZnO PhCS ($f > 50\%$), that in turn drives down the size of the features to be produced in the experiment.

A band-structure calculation technique for the asymmetric geometry like ours was proposed in Ref. 3. The authors of Ref. 3 proposed to use a supercell where ···-substrate-PhCS-air-substrate-PhCS-air-··· is periodically repeated in the z direction. Special care needs to be exercised in order to avoid unphysical solutions that correspond to the guided modes in the substrate layers bounded by air and a PhCS. In our simulation we constructed a different supercell by combining the structure and its mirror image (shown in Fig. 1) for the photonic band calculation.[29] Our choice of the unit cell is motivated by the following. Due to a particular arrangement of the layers in our supercell, there exists an artificial symmetry—reflection plane Σ_{sc} in Fig. 1. Therefore, there is an artificial classification of the modes into symmetric and antisymmetric, as it is schematically shown in Fig. 2. This property provides a way to control the precision of the band-structure calculation. Indeed, only for the PhCS-guided modes (with eigenfrequencies outside of the air and substrate
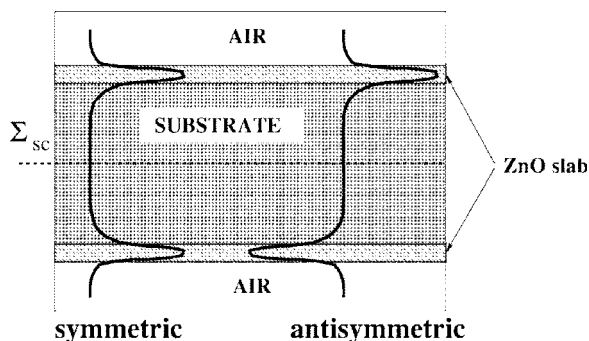
FIG. 2. Reflection symmetry allows for solutions symmetric and antisymmetric with regard to reflection in Σ_{sc}. This artificial symmetry helps us to separate the guided modes from the leaky ones.
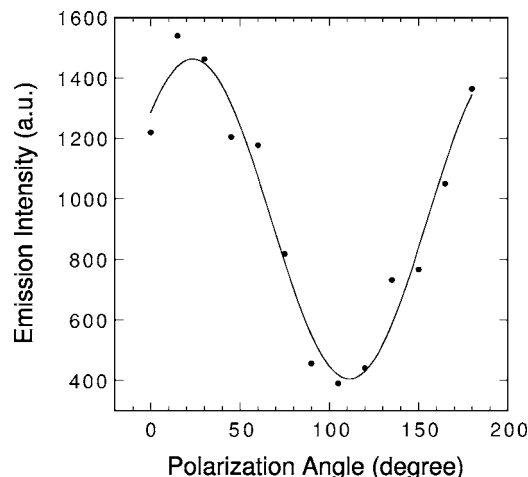

FIG. 3. Experimentally measured emission intensity from a 600-nm-thick ZnO film as a function of polarization angle. The maximum intensity at about 25° corresponds to E-field polarization parallel to the plane of the film (TE polarization).

light cones), and only when the thicknesses of air (t_a) and substrate (t_s) layers are chosen to be sufficiently large, the eigenfrequencies of the Σ_{sc}-symmetric and Σ_{sc}-antisymmetric modes are nearly degenerate. This can be seen from Fig. 2: there should be no difference in eigenenergy between the functions when the value of the eigenfunction is close to zero at the (i) Σ_{sc} plane and (ii) the top/bottom of the supercell. The second condition arises because of the periodicity in the vertical direction—the top/bottom of the supercell is also a middle plane that separates two closest PhCS layers.

Furthermore, one may think that the doubling of the cell size should increase the computation time. However, at least for a PhCS with a hexagonal symmetry, Σ_{sc} contains a center of inversion. The latter allows us to perform the photonic band-structure calculation, assuming that inversion symmetry shortens the calculation time (of one symmetry) by a half. In all simulations reported below, we checked the consistency of the results with the procedure outlined above, then studied the band structure of the modes outside of the substrate (more restrictive) light cone.

III. PHOTONIC MODE CLASSIFICATION: POLARIZATION

We measured the polarization of ZnO emission intensity from a 600-nm-thick ZnO film on a sapphire substrate. The c axis of ZnO is perpendicular to the surface of the film. ZnO is optically excited by the third harmonic of a mode-locked Nd:YAG (yttrium aluminum garnet) laser (355 nm, 10 Hz, 20 ps). A cylindrical lens ($f=100$ mm) is used to focus the pump beam to a strip normal to the edge of the sample. The emission was collected from the edge of the sample at 1 μJ pump pulse energy. The pump area was about 2 mm $\times 50$ μm. Figure 3 clearly demonstrates that the emission is strongly polarized with the electric field parallel to the film (TE polarization).[27,28] Because the emission in the ZnO thin film is predominantly TE polarized we need to consider only the TE-polarized photonic modes. This motivates a detailed analysis of the polarization of the modes in the experimentally relevant PhCS. Reference 30 describes an experimental technique designed to measure the degree of polarization of a photonic mode. In ZnO PhCS this approach cannot be used because the correspondent Bragg length is of the same order

as the attenuation length due to material reabsorption. Below we will use theoretical band-structure calculation to study mode polarization.

In Fig. 4 we show an example of the calculated photonic band structure. Air light-cone boundary, $\omega=ck_{\parallel}$, and substrate light-cone boundary, $\omega=(c/n_s)k_{\parallel}$, are shown with dash-dot and dashed lines, respectively. The presence of a sapphire cone makes guiding at the Γ point impossible and limits any band gap to $a/\lambda < 0.325$. For PhCS laser operation we need to overlap a photonic band gap with a gain spectrum of ZnO, 380 nm $< \lambda < 400$ nm. Consequently, the lattice constant in the hexagonal air-hole pattern of PhCS has an upper bound of $a < 130$ nm. To fabricate such small features we used the FIB etching technique.[21]

Since the presence of the substrate removes the symmetry with respect to reflection in the PhCS middle plane (Σ in Fig. 1), one cannot separate the modes into two independent classes and consider them separately. This separability was crucial for obtaining a sizable PBG in a photonic membrane (or strictly two-dimensional structures). For comparison, we
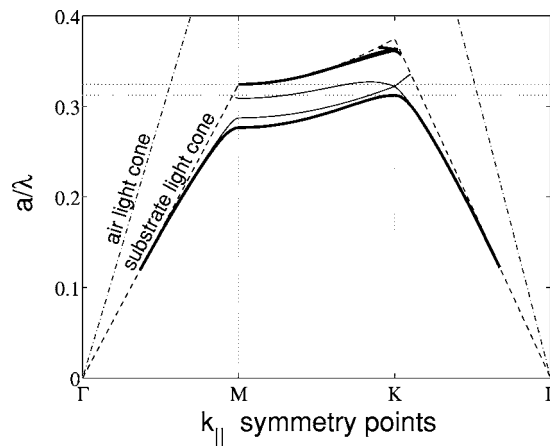

FIG. 4. Calculated band structure of ZnO photonic crystal slab air cylinder radius $r/a=0.25$ and slab thickness $t/a=1.4$. The refractive indices for ZnO and sapphire are 2.35 and 1.78. The thin and thick lines represent the TM- and TE-polarized modes, respectively.
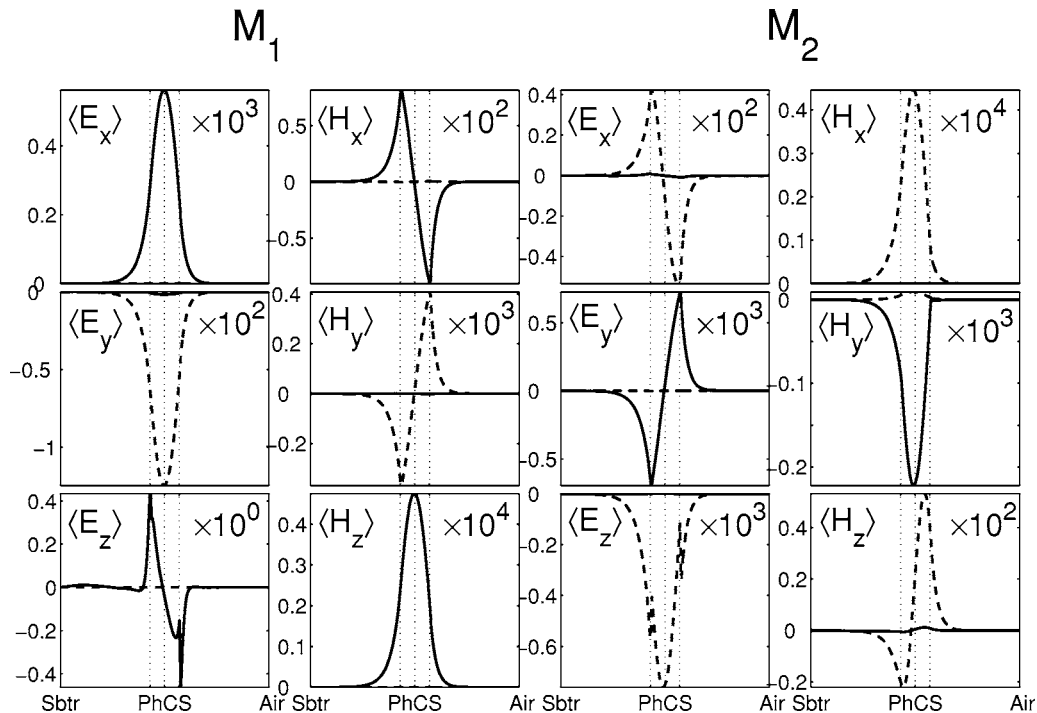
FIG. 5. Integrated according to Eq. (1) the x, y, and z components of the electric, E, and magnetic, H, fields. The solid/dashed lines represent the real/imaginary part of the field. The first/second two columns correspond to the first/second mode of Fig. 4 taken for $k_\parallel$ at the M-symmetry point. The same normalization is used for all field components, so that their values can be compared. Mode M_1/M_2 shows a pronounced TE/TM polarization.

calculated the band structure of the system with the same parameters as in Fig. 4 but the sapphire substrate was replaced by air. The obtained dispersions looked qualitatively similar to the ones in Fig. 4, so that it was possible to make band-to-band correspondence. This has been used previously to justify the existence of PBG in the spectrum of TE modes.[7] In our case the refractive index of the substrate is quite large; moreover it may even become comparable to the effective index of PhCS as the patterning of ZnO film with original refractive index $n_{ZnO}=2.35$ will reduce it to just a little above that of the sapphire. These considerations warrant an in-depth analysis of the mode polarizations.

In order to determine the degree of polarization of the electromagnetic eigenmodes of PhCS, we studied

$$\langle F(z)\rangle = \int F(x,y,z)dxdy, \qquad (1)$$

where F represents the x, y, or z component of the electric or magnetic field. Figure 5 shows these quantities for the first two bands taken at the M-symmetry point of Fig. 4. It is clearly seen that the first (the lowest-frequency) mode M_1 is strongly TE polarized: E_x, E_y, and H_z are more than one order of magnitude larger than the other components. Furthermore, as discussed above dominant components are nearly symmetric with respect to the middle plane of the PhCS, whereas H_x, H_y, and E_z are close to antisymmetric. The deviation from the perfect symmetry is entirely due to the presence of the sapphire substrate. Comparing the second mode M_2 to the previous case one notices that the polarization of the field has changed to the opposite—M_2 is predominantly TM polarized.

An increase in the order of the band does lead to an enhancement of polarization mixing. However, as we will see in more detail below, the substrate light-cone condition restricts the involvement of higher-order bands. We checked the polarization of the lowest six bands in several $k_\parallel$ points and found that in all relevant cases certain symmetry, TE or TM, can be assigned to each band. Therefore, despite the highly asymmetric claddings (sapphire versus air) and relatively small refractive index contrast between PhCS ($n_{eff} \sim 2.1$) and the substrate ($n_s=1.78$), the mixing of the polarizations in the low-order photonic bands is limited. From now on we will ignore TM-polarized bands. In the next section we will systematically study the effect of the structural parameters on the width of the PBG in the spectrum of TE (see thick solid lines in Fig. 4) modes.

IV. PHOTONIC BAND-GAP OPTIMIZATION

We intend to optimize the following three parameters that can be controlled in the FIB etching technique:[21] (i) PhCS thickness, t_{PhCS}, (ii) air-hole radius, r (related to the filling fraction f), and etch depth, t_e. Due to linear nature of Maxwell equations, we normalize all parameters to the value of lattice constant, a. Our goal is to maximize the relative (normalized to the center frequency) PBG width. Once this is achieved, we can overlap the PhCS gap with the emission spectrum of ZnO by choosing appropriate a. From the experimental prospective it is difficult to reproduce extremely small structural features, therefore we prefer to have PBG at high values of a/λ if possible.

Figure 6 shows the results of our simulation. In panel (a) we plot the position and relative width of the PhCS as we vary r/a within the range of 0.18–0.30, and keep t_{PhCS}/a
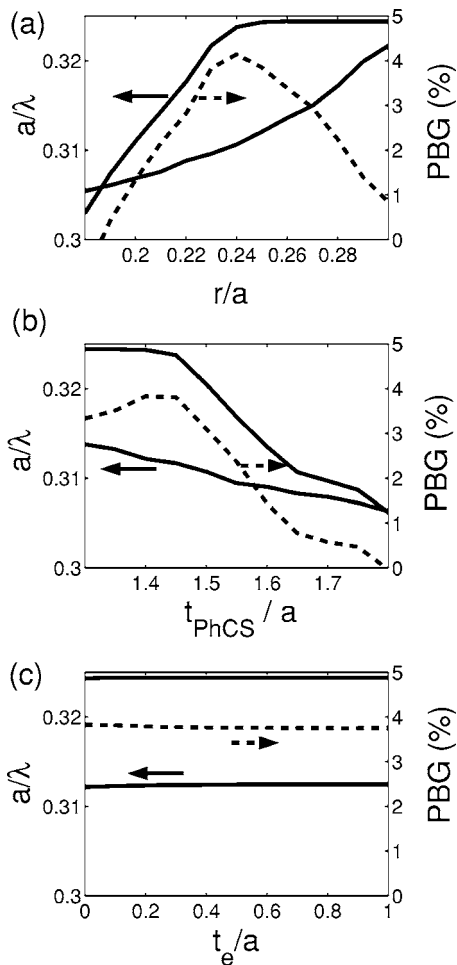
FIG. 6. The position and relative size of the photonic band gap for PhCS with variable structural parameters. (a) $t_{PhCS}/a=1.4$, $t_e=0$; (b) $r/a=0.25$, $t_e=0$; and (c) $r/a=0.25$, $t_{PhCS}/a=1.4$. $n_{ZnO}=2.35$ and $n_s=1.78$ were used in the calculation. The left vertical axes should be used with solid lines, which represent the edges of the PBG. The dashed lines and the right vertical axes show the relative size of the gap.

$=1.4$ and $t_e=0.0$. This corresponds to a change in the pattern filling fraction from $f=0.88$ to $f=0.67$. One can clearly see that there exists a PBG maximum at $r/a \simeq 0.24$ (or $f \simeq 0.79$). This effect has a clear physical interpretation: at large filling fractions (small r/a) the index contrast within the PhCS is small, therefore band splitting, as well as PBG, is small. At small filling fractions, the waveguiding becomes poor, furthermore the decrease of the effective refractive index of the photonic layer leads to a shift of the PBG as a whole to higher frequency. Eventually, at $r/a \simeq 0.26$ the top of the gap is set not by the higher-order guided mode but by $a/\lambda \simeq 0.324$ at the light cone when $k_{\parallel}$ is at the M point (see Fig. 4). In reality, above this frequency the guided modes will always be coupled to some leaky modes inside the light cone. This phenomenon results in a plateau of the upper band-gap edge for $r/a=0.26-0.30$. Consequently, PBG disappears at $r/a>0.30$. For the air holes with such a large radius, the effective refractive index of the PhCS $n_{eff} \simeq 1.87$ approaches that of the substrate.

Figure 6(b) presents the effect of the photonic layer thickness, t_{PhCS}, on the PBG. With the increase of t_{PhCS} we also observe a maximum. For samples thinner than the cor-

respondent wavelength, the eigenmodes of the system substantially "spill" into the air and (mostly) the substrate. Consequently, the effective index of the PhCS becomes comparable to n_s so that the PBG lies at higher frequencies. The light cone leads to the plateau of the upper band-gap edge as in the case of large r/a in Fig. 6(a). For very thick photonic layers, $t_{PhCS}/a>1.5$, the gap closes again. This occurs due to a stronger dependence of the upper band-edge frequency on the effective refractive index of the PhCS. Indeed, as n_{eff} is increased the band forming the upper edge of the PBG develops the kinks close to the light cone, which leads to the reduction of the PBG, as seen in Fig. 6(b). As a result of these dependences, the size of the gap can be maximized at $t_{PhCS}/a \simeq 1.45$.

The possibility of improving the guiding properties of the photonic layer by extending the air holes into the substrate was discussed in Ref. 31. Indeed, removing a part of the substrate material lowers its refractive index and achieves a partial effect of "undercutting." However, the fact that PBG in our case lies close to the light cone has a significant effect. An increase in t_e results in the decrease of the effective refractive index experienced by a guided mode, because it extends into the substrate. Therefore the eigenfrequency of the mode increases and may enter the light cone.[32] This is exactly what happens in our system, as shown in Fig. 6(c). As t_e is increased the upper edge of the PBG becomes defined by the position of the substrate light cone at the M k-point (Fig. 4), whereas the mode that defines the lower edge of the PBG is more confined to the PhCS and, therefore, is less sensitive to the effect of t_e. As a result, Fig. 6(c) shows a weak dependence on the etch depth.

As we discussed in the previous section our calculation of the photonic band gap relies on the possibility of separating the photonic bands based on their polarization. To check the consistency of this assumption we calculated the ratios between in-plane and normal components of the electric fields for various structural parameters. In Fig. 7, we show the polarization ratios calculated for the lowest four bands at two $k_{\parallel}$ vectors (M and K k-points). As the structural parameters are varied, the polarization of the modes is preserved. The most noticeable change occurs with the increase of r/a in Fig. 7(a). This is due to significant modification of the band structure that occurs in this case. Notwithstanding, the modes still remain strongly polarized, justifying our methodology.

V. DISCUSSION AND CONCLUSION

In order to simulate the realistic structures to be realized in the experiment,[21] we modified supercell technique[3] within plane-wave expansion method for the photonic band-structure calculation.[29] We constructed a symmetric supercell with the doubled size, Fig. 1. The induced degeneracy of eigenvalues provides a convenient way to verify the self-consistency of the calculation.

The substrate with high refractive index was expected to significantly mix the polarization of eigenmodes of the PhCS. However, our calculations demonstrate that although the substrate induces asymmetry of wave functions (Fig. 5),
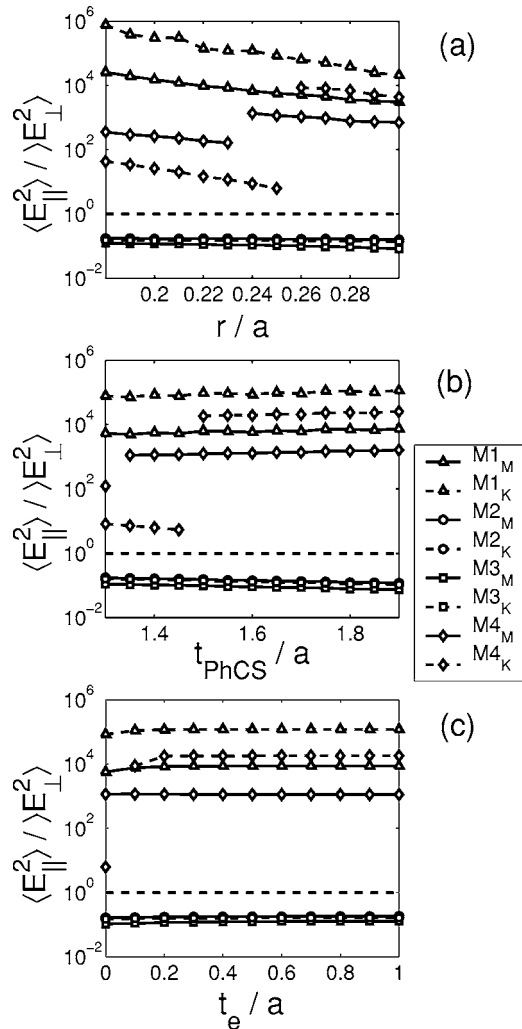
FIG. 7. The degree of polarization of the modes calculated for $k_\parallel$ in the M (solid lines) and K (dashed lines) k points. The modes belonging to the lowest four bands are considered. Cases (a)–(c) correspond to those of Fig. 6. $\langle \cdots \rangle$ denotes an integration over x and y coordinates. Discontinuities in the curves occur when the order of bands changes.

they remain strongly TM or TE polarized for low-order bands. High filling fraction air-hole-in-ZnO-matrix geometry can possess a complete PBG for TE bands, meanwhile, ZnO film with c axis along the growth direction emits mainly into TE-polarized modes. This enabled us to build an UV PhCS laser.[21] In the photonic band-structure calculation we find the optimum set of parameters for maximum PBG,

$$\frac{r}{a} \simeq 0.24, \quad \frac{t_{\mathrm{PhCS}}}{a} \simeq 1.45, \quad \frac{t_e}{a} \simeq 0.0. \quad (2)$$

These parameters are significantly different from the typical parameters for IR PhCS. This is due to several factors: (i) the presence of the sapphire substrate breaks the vertical symmetry of the PhCS, (ii) the refractive index contrast of ZnO/sapphire is lower than that of InP/air usually used in IR PhCS, and (iii) to preserve guiding in the photonic layer the filling fraction and the thickness of ZnO PhCS need to be significantly increased. This in turn explains the relatively small PBG of about 5% that can be obtained in the ZnO PhCS on sapphire.

Overlapping the photonic band gap with the emission spectrum of zinc oxide required precise control of the designed pattern with

$$a \simeq 123 \text{ nm}, \quad t_{\mathrm{PhCS}} \simeq 180 \text{ nm}, \quad t_e \simeq 0 \text{ nm}, \quad r \simeq 30 \text{ nm}. \quad (3)$$

This has been achieved with the FIB etching technique. In order to avoid an additional damage to the PhCS we did not attempt to remove the substrate, in other words, experimentally we preferred $t_e = 0$. The maximum relative width of the PBG that can be achieved via optimization is 5%. This is significantly smaller than what is being used in the membrane (air-bridge) geometry[5,15,16] or in the case of low refractive index substrate.[7,26] Narrow gap makes it difficult to align an intentionally introduced defect mode inside the PBG. However, there are always some defect modes with frequencies inside the PBG formed by small disorder unintentionally introduced in the fabrication process. These are the lasing modes observed in our experiment.

[1]R. D. Meade, A. Devenyi, J. D. Joannopoulos, O. L. Alerhand, D. A. Smith, and K. Kash, J. Appl. Phys. **75**, 4753 (1994).
[2]P. L. Gourley, J. R. Wendt, G. A. Vawter, T. M. Brennan, and B. E. Hammons, Appl. Phys. Lett. **64**, 687 (1994).
[3]S. G. Johnson, S. Fan, P. R. Villeneuve, J. D. Joannopoulos, and L. A. Kolodziejski, Phys. Rev. B **60**, 5751 (1999).
[4]T. F. Krauss, R. M. De La Rue, and S. Brand, Nature (London) **383**, 699 (1996).
[5]O. Painter, R. K. Lee, A. Scherer, A. Yariv, J. D. O'Brien, P. D. Dapkus, and I. Kim, Science **284**, 1819 (1999).
[6]S. Noda, A. Chutinan, and M. Imada, Nature (London) **407**, 608 (2000).
[7]E. Chow et al., Nature (London) **407**, 983 (2000).
[8]Y. Akahane, T. Asano, B. Song, and S. Noda, Nature (London) **425**, 944 (2003).
[9]M. Soljacic and J. D. Joannopoulos, Nat. Mater. **3**, 211 (2004).
[10]*Photonic Crystals and Light Localization in the 21st Century*, edited by C. M. Soukoulis (Kluwer Academic, Dordrecht, 2001).
[11]M. Imada, S. Noda, A. Chutinan, T. Tokuda, M. Murata, and G. Sasaki, Appl. Phys. Lett. **75**, 316 (1999).
[12]H. Benisty et al., IEEE J. Lightwave Technol. 17, 2063 (1999).
[13]J. Hwang, H. Ryu, D. Song, I. Han, H. Song, H. Park, Y. Lee, and D. Jang, Appl. Phys. Lett. **76**, 2982 (2000).
[14]M. Loncar, T. Yoshie, A. Scherer, P. Gogna, and Y. M. Qiu, Appl. Phys. Lett. **81**, 2680 (2002).
[15]H.-Y. Ryu, S.-H. Kwon, Y.-J. Lee, Y.-H. Lee, and J.-S. Kim, Appl. Phys. Lett. **80**, 3476 (2002).
[16]H. G. Park, S. H. Kim, S. H. Kwon, Y. G. Ju, J. K. Yang, J. H. Baek, S. B. Kim, and Y. H. Le, Science **305**, 1444 (2004).
[17]S. G. Johnson, S. Fan, A. Mekis, and J. D. Joannopoulos, Appl. Phys. Lett. **78**, 3388 (2001).
[18]J. Vučković, M. Lončar, H. Mabuchi, and A. Scherer, Phys. Rev. E **65**, 016608 (2001).
[19]K. Srinivasan and O. Painter, Opt. Express **10**, 670 (2002).
[20]M. Notomi, H. Suzuki, and T. Tamamura, Appl. Phys. Lett. **78**, 1325 (2001).
[21]X. Wu, A. Yamilov, X. Liu, R. P. H. Chang, and H. Cao, Appl. Phys. Lett. **85**, 3657 (2004).
[22]Y. S. Park, C. W. Litton, T. C. Collins, and D. C. Reynolds, Phys. Rev. **143**, 512 (1966).
[23]X. Wu, A. Yamilov, X. Liu, R. P. H. Chang, and H. Cao (unpublished).
[24]X. Liu, A. Yamilov, X. Wu, J. Zheng, H. Cao, and R. P. H. Chang, Chem. Mater. **16**, 5414 (2004).
[25]M. Qiu, Phys. Rev. B **66**, 033103 (2002).
[26]C. Monat et al., Appl. Phys. Lett. **81**, 5102 (2002).
[27]S. F. Yu, C. Yuen, S. P. Lau, and W. J. Fan, IEEE J. Quantum Electron. **40**,

406 (2004); S. F. Yu, C. Yuen, S. P. Lau, W. I. Park, and G.-C. Yi, Appl. Phys. Lett. **84**, 3241 (2004).

[28]H. Cao, Y. G. Zhao, H. C. Ong, S. T. Ho, J. Y. Dai, J. Y. Wu, and R. P. H. Chang, Appl. Phys. Lett. **73**, 3656 (1998).

[29]S. G. Johnson and J. D. Joannopoulos, Opt. Express **8**, 173 (2001).

[30]D. Labilloy, H. Benisty, G. Weisbuch, T. F. Krauss, R. Houdre, and U. Oesterle, Appl. Phys. Lett. **71**, 738 (1997).

[31]R. Ferrini, R. Houdré, H. Benisty, M. Qui, and J. Moosburger, J. Opt. Soc. Am. B **20**, 469 (2003).

[32]As it is discussed in Ref. 7, altering the substrate (by extending the air hole into it) also changes the position and the shape of the correspondent light cone. This effect was not taken into account in our calculation. We believe it should not substantially change the result of our optimization. Furthermore, to avoid the degradation of the optical quality of ZnO PhCS, $t_e=0$ was used in the experiment (Ref. 21).